Towards on-chip implementation of fast delay-based reservoir computing using semiconductor ring lasers

Romain Modeste Nguimdo, Guy Verschaffelt, Jan Danckaert, and Guy Van der Sande

Applied Physics Research Group, Vrije Universiteit Brussel, 1050 Brussels Belgium
Email: Romain.Nguimdo@vub.ac.be, guy.van.der.sande@vub.ac.be

Abstract—In this contribution, we investigate the computational abilities of semiconductor ring lasers with optical delayed feedback for machine learning tasks. We benchmark our system on a chaotic time series prediction task. The results show that, as other types of lasers, good performance can be obtained in a broad range of the key parameters. In particular, we find that fast processing speed of 0.5 GSample/s can be achieved. This is obtained even for an overall delay loop of 2 ns. With this short delay, it is possible to implement this reservoir computing schemes on chip as both the semiconductor ring lasers and such a short delay can be easily implemented on the same chip.

1. Introduction

Reservoir computing (RC) is a computational paradigm inspired by the way that the brain processes the information. It can potentially perform computationally hard tasks such as pattern recognition, time series prediction and classification at which the brain excels [1–4]. Unlike traditional computers where the information processing is typically handled sequentially, the RC concept is based on the computational power associated with complex nonlinear transient motion developed in a high dimensional nonlinear system [5]. A reservoir computing consists of an input layer, a reservoir and an output layer. The reservoir structure typically considers $10^2 - 10^3$ randomly connected nonlinear dynamical nodes which allow to reach the high dimensionality necessary to achieve a good performance [5, 6]. While this high number of nodes typically renders the experiments more difficult, L. Appeltant et al. recently demonstrated that the architecture of reservoir computing scheme can be drastically simplified by replacing the entire reservoir nodes by a single dynamical nonlinear node subject to delayed-feedback [7]. This work paved the way for several experimental implementations including electro-optical [8–10] and all-optical [11–13] schemes. These schemes make use of the great potential of light to achieve fast data processing speeds (order of MSample/s for time series prediction).

Recently, we have numerically shown that much faster information processing speeds (order of GSample/s for time series prediction) can be achieved in lasers even using very short delay lengths, thanks to the fast phase dynamics and optical injection which couples such fast phase dynamics to the intensity dynamics [14]. However, the RC systems based on delay dynamics discussed in the literature are designed by coupling many different stand-alone components (e.g. delay fibers, external mirrors, polarization controllers, semiconductor lasers, etc..) which lead to bulky, lack of long-term stability, non-monolithic systems. These drawbacks motivate to investigate devices designed in a compact way and integrated on chip.

Semiconductor ring lasers (SRLs) or micro-ring lasers appear as promising candidates for compact and integrated devices for delay-based RCs since they are scalable, do not require distributed feedback or distributed Bragg reflector mirrors to implement the feedback and multiple output ports can easily be implemented. In addition, they can easily be implemented with other photonic components on the same chip. The fact that several feedback configurations can be achieved in SRLs allows for more variability in the system design. In particular the implementation of double feedback configuration can improve the memory capacity of the system [15]. However, due to the existence of two counter propagating modes interacting both in a linear and nonlinear fashion, it is not easy to make a quick estimate of their computational power.

In this contribution, we numerically investigate the computational performance of SRLs considering different feedback configurations including cross- and self-feedback configurations. We mainly consider a short delay loop and use a chaotic time series prediction as the benchmark to explore different parameter sets for good performance. The results indicate that good results i.e. small prediction errors can be obtained for any of the two configurations considered even in the presence of realistic noise in the laser.

2. Model

We consider a SRL with double optical self- and cross-feedback [16–20] extended to include the optical injection of data. Taking into account the effect of spontaneous emission noise, the dynamics of single-longitudinal SRLs with feedback in the two modes and injection in one mode can be described, in terms of the mean-field slowly varying complex amplitudes of the electric field associated with the two propagating modes $E_{cw} = |E_{cw}|e^{i\varphi_{cw}}$ and

$E_{ccw} = |E_{ccw}|e^{i\varphi_{ccw}}$, and the carrier number $\mathcal{N}$ as:

$$\dot{E}_{cw} = \kappa(1+i\alpha)\left[\mathcal{G}_{cw}N - 1\right]E_{cw} - (k_d + ik_c)E_{ccw} + \eta_{cw}\mathcal{F}_{cw}(t) + \sqrt{D_{cw}}\xi_{cw}(t) + k_{inj}\mathcal{E}_{inj}(t), \quad (1)$$

$$\dot{E}_{ccw} = \kappa(1+i\alpha)\left[\mathcal{G}_{ccw}N - 1\right]E_{ccw} - (k_d + ik_c)E_{cw} + \eta_{ccw}\mathcal{F}_{ccw}(t) + \sqrt{D_{ccw}}\xi_{ccw}(t), \quad (2)$$

$$\dot{\mathcal{N}} = \gamma\left[\mu - \mathcal{N}\left(1 + \mathcal{G}_{cw}|E_{cw}|^2 + \mathcal{G}_{ccw}|E_{ccw}|^2\right)\right], \quad (3)$$

where the parameters are the linewidth enhancement factor α, renormalized bias current μ, field decay rate κ, carrier inversion decay rate γ, feedback strengths η_{cw} and η_{ccw}, and the backscattering coefficients $k_d + ik_c$ where k_c and k_d are the conservative and the dissipative couplings, respectively. The differential gain functions are given by $\mathcal{G}_{cw} = 1 - s|E_{cw}|^2 - c|E_{ccw}|^2$ and $\mathcal{G}_{ccw} = 1 - s|E_{ccw}|^2 - c|E_{cw}|^2$ where s and c account for the phenomenological self- and cross-saturations, respectively. $\mathcal{F}_{cw}(t)$ and $\mathcal{F}_{ccw}(t)$ are the feedback terms which can be explicitly defined depending on the feedback configuration. The feedback can be implemented by injecting back a part of the output signal of one directional mode either in the same direction (self-feedback configuration) or in the opposite direction (cross-feedback configuration). Note that one directional mode (single feedback) or the two directional modes simultaneously (double feedback) can be subjected to feedback. For a double cross-feedback configuration, $\mathcal{F}_{cw}(t) = E_{ccw}(t - T_{ccw})e^{-i\omega_0 T_{ccw}}$ and $\mathcal{F}_{ccw}(t) = E_{cw}(t - T_{cw})e^{-i\omega_0 T_{cw}}$ where ω_0 is solitary laser frequency, T_{cw} and T_{ccw} are delay times and $\omega_0 T_{cw}$ and $\omega_0 T_{ccw}$ are the constant feedback phases. For a double self-feedback configuration, $\mathcal{F}_{cw}(t) = E_{cw}(t - T_{cw})e^{-i\omega_0 T_{cw}}$ and $\mathcal{F}_{ccw}(t) = E_{ccw}(t - T_{ccw})e^{-i\omega_0 T_{ccw}}$.The fourth terms at the right hand side of Eqs. (1) and (2) represent the effect of spontaneous emission noise coupled to the CW/CCW modes. It can be explicitly written as $D_{cw,ccw} = D_m(\mathcal{N} + G_0\mathcal{N}_0/\kappa)$ where D_m is the noise strength and can differ from one mode to another although we consider identical values in this study, G_0 is the gain parameter and $\mathcal{N}_0$ is the transparent carrier density. $\xi_i(t)$ $(i = cw, ccw)$ are two independent complex Gaussian white noises with zero mean and correlation $\langle \xi_i(t)\xi_i^*(t')\rangle = \delta(t - t')$. The last term in Eq. (1) is the injected signal containing the task to be processed (which here has been injected in the CW mode), k_{inj} being the injection strength. This term results from the input signals after a pre-processing.

Typical benchmark tasks to test the RC performances include Signal Classification, Nonlinear Channel Equalization, Isolated Spoken Digit Recognition and Santa-Fe Prediction [5,8–10]. The latter requires both a nonlinearity and a memory and will be adopted here. The Santa-Fe data are intensity time series experimentally recorded from a far-infrared laser operating in a chaotic state [21]. Our Santa-Fe data set contains 10000 points and we use the first 4000 points. Of these 4000 points, the first 75% is used for training while the remaining 25% is used for testing. The target for this task is to predict the next sample in the chaotic time trace before it has been injected into the reservoir computer (one-step ahead prediction). In practice, these data can be optically injected into the reservoir using a Mach-Zehnder modulator [12–14]. Thus, before being fed into the reservoir, the original data are first multiplied with a random mask. We assume a random mask with four predefined discrete levels $(0, 0.25, 0.75, 1)$ [22]. Other ways to construct the mask have been also suggested [23]. The data with mask is used to modulate a continuous-wave input power of a Mach-Zehnder modulator via its radio-frequency electrode. Subsequently, the Mach-Zehnder modulator output given by Eq. (4) is injected in the CW of the SRL. The mask is generated so that it is constant over the virtual node's separation Θ and periodic over one delay time T_{cw}. The number of the virtual nodes $N = T_{cw}/\Theta$ where Θ depends on the damping intrinsic time scale. Explicitly $\mathcal{E}_{inj}(t)$ can be written as

$$\mathcal{E}_{inj}(t) = \frac{|\mathcal{E}_0|}{2}\left\{1 + e^{i[S(t)+\Phi_0]}\right\}e^{i\Delta\omega t} \quad (4)$$

where $|\mathcal{E}_0|$ is the amplitude of the injection. $S(t)$ is the resulting signal from the Santa-Fe data convoluted with the random mask. It is set in this study so that $0 \leq S(t) \leq \pi$.

3. Results

We use [16, 18]: $\alpha = 3.5$, $s = 0.005$, $c = 0.01$, $\kappa = 100$ ns^{-1} (corresponding to the photon lifetime of 10 ps), $\gamma = 0.2$ ns^{-1}, $\omega_0 T_{cw} = \omega_0 T_{ccw} = 0$, $k_d = 0.033$ ns^{-1}, $k_c = 0.44$ ns^{-1}, $N = 100$ nodes, $|\mathcal{E}_0| = 2$ and $\Phi = 0$ and $\kappa_{inj} = 30$ ns^{-1}. In addition, we also consider the noise parameters as [24]: $D_{cw} = D_{ccw} = 5 \times 10^{-4}$ ns^{-1}, $G_0 = 10^{-12}$ m^{3}s^{-1} and $\mathcal{N}_0 = 1.4 \times 10^{24}$ m^{-3}. Other parameters, i.e T_{cw}, T_{ccw}, μ, η_{cw}, η_{ccw} are set in the figure captions. The system performance is characterized by the mean of the Normalized Mean Square Error (NMSE). The reservoir output signal is recorded as $|E_{cw}(t)|^2$. The system is assumed as computationally suitable when the NMSE stays below 10%.

In ref. [14], it is shown that the node's separation can be freely chosen between the fast time scale and the relaxation oscillation period $\tau_{R0} \approx 2\pi/\sqrt{2(\mu - 1)\gamma\kappa}$. We consider μ as the control parameter as it can be freely changed in the compact experimental setup. Figure 1 depicts the NMSE as function of μ for various parameters. More precisely in Fig. 1 (a, c), we evaluate the NMSE as a function of the μ for two values of Θ: $\Theta = 20$ ps (•) and $\Theta = 200$ ps (■), considering $\eta_{cw} = \eta_{ccw} = 10$ ns^{-1} for double cross-feedback configuration (a) and $\eta_{cw} = \eta_{ccw} = 20$ ns^{-1} self-feedback configuration (c) schemes. In both configurations, the results indicate that $\Theta = 20$ ps leads a better performance (i.e small values of NMSE) than $\Theta = 200$ ps in the whole range of μ explored. For double cross-feedback configuration, NMSE gradually decreases and approaches the same values at high pump currents for the two values of Θ [Fig. 1 (a)]. For example, for $\mu = 1.8$, NMSE is ≈ 0.05 and 0.08 for $\Theta = 20$ ps and $\Theta = 200$ ps, respectively. For double self-feedback configuration, we use $\eta_{cw} = \eta_{ccw} = 20$ ns^{-1}. The

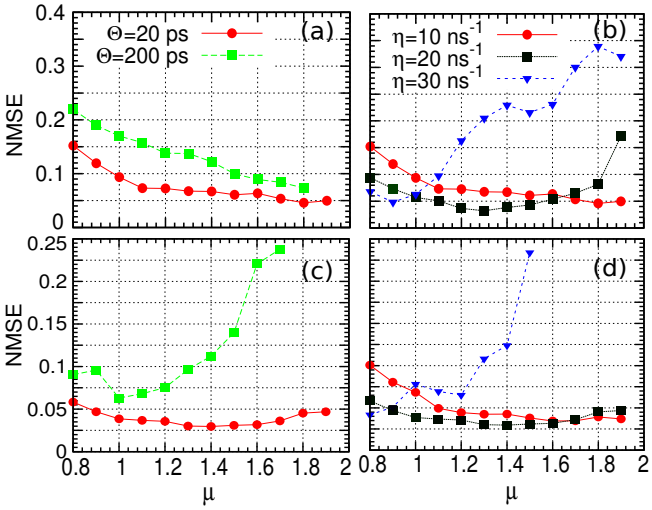

Figure 1: NMSE for SRL with double cross-feedback (a, b) and double self-feedback (c, d): (a) $\eta = \eta_{cw} = \eta_{ccw} = 10$ ns^{-1}, (c) $\eta = \eta_{cw} = \eta_{ccw} = 20$ ns^{-1} and (b, d) $\Theta = 20$ ps. The data are input and read out in CW.

results show very good system performance (the smallest error of 0.0229 is obtained at $\mu \approx 1.4$) for $\Theta = 20$ ps in the whole range of μ while the regions of small NMSE are confined around the threshold pump current for $\Theta = 200$ ps, due to the fact that the rest state becomes unstable. In fact, for $\Theta = 200$ ps i.e $T_{cw} = N\Theta = 20$ ns the rest state becomes unstable above $\mu = 1.1$ while for $\Theta = 20$ ps i.e $T_{cw} = N\Theta = 2$ ns, it remains stable. Globally, we have found that the self-feedback configuration performs better than the cross-feedback configuration. This is due to the fact that, in the cross-feedback configuration, while information is injected in one mode, it needs to be passed through the other mode before it can be mixed with new information in the original mode. We have checked that similar results can be obtained in both configurations when the data are read out as $|E_{cw}|^2 + |E_{ccw}|^2$ instead of $|E_{cw}|^2$.

It is important to note that small values of Θ are particularly desirable as they allow for shorter delay lengths and consequently faster information processing. In addition, short delay lengths are suitable for on-chip implementations as they will not consume a lot of wafer space. Thus, considering $\Theta = 20$ ps we further explore, in both configurations, the optimized parameters for small prediction errors by estimating the NMSE as a function of μ for different values of the feedback strengths [Fig. 1 (b, d)]. In particular, the NMSE is smaller than 0.05 in a broad range of μ in both configurations for $\eta = \eta_{cw} = \eta_{ccw} = 20$ ns^{-1} even with a strong noise involved in the reservoir. However, further increase of the feedback strength to $\eta = \eta_{cw} = \eta_{ccw} = 30$ ns^{-1} worsens the NMSE except for the cases for which the system operates close to the threshold. It should be indeed noted that the increase of the feedback strength accordingly enhances the amplitude of the signals below, but close to the threshold (this was checked through the computation of the power spectra). That is why in Fig. 1 (b, d), the NMSE gradually decreases as the feedback strength increases for $\mu \lesssim 1$. The degradation of the NMSE for $\mu > 1$ confirms the fact that more complex dynamics are generated for strong feedback strengths above the threshold.

Remarkably, the independence of the phase relaxation to the pump current as shown in ref. [14] also justifies the fact that in Fig. 1, the NMSE does not change significantly for $\Theta = 20$ ps in the whole range of μ. In particular, the good system performance obtained below the threshold further confirms that the phase dynamics rather than the intensity dynamics plays an important role in the computational capacities of our system. With $\Theta = 20$ ps and $N = 100$, the processing speed is 0.5 GSample/s. While the noise in the readout layer has not been considered here, we refer to our previous work which showed that good performance can be obtained considering readout noise [14].

4. Conclusions

We have investigated the computational performance of SRLs with delayed optical feedback for information processing. Using chaotic time series prediction as the benchmark and NMSE as the performance metric, we identified a broad range of the pump current in which good performance can be achieved in both configurations. In particular, we have considered small values of the node separation to obtain good performance with very short delay times. We have also found that feedback strengths and the pump currents can be adjusted such as to obtain good performance below and above the laser pump current threshold.

Acknowledgments

The authors acknowledge the Research Foundation Flanders (FWO) for project support, the Research Council of the VUB and the Interuniversity Attraction Poles program of the Belgian Science Policy Office, under grant IAP P7-35 photonics@be.

References

[1] W. Maass, T. Natschläger, H. Markram, "Real-time computing without stable states: a new framework for neural computation based on perturbations," Neural Comput. **14**, 2531 (2002).

[2] H. Jaeger and H. Haas, "Harnessing nonlinearity: predicting chaotic systems and saving energy in wireless communication," Science **304**, 78 (2004).

[3] D. Verstraeten, B. Schrauwen, M. D'Haene, and D. Stroobandt, "An experimental unification of reservoir computing methods," Neural Networks **20**, 391 (2007).

[4] J. J. Steil "Backpropagation-decorrelation: Online recurrent learning with O(N) complexity," In Proceedings of IJCNN 04 **1**, 843-848 (2004).

[5] K. Vandoorne, W. Dierckx, B. Schrauwen, D. Verstraeten, R. Baets, P. Bienstman, and J. Campenhout, "Towards optical signal processing using photonic reservoir computing," Opt. Express **16**, 11182 (2008).

[6] K. Vandoorne, P. Mechet, T. V. Vaerenbergh, M. Fiers, G. Morthier, D. Verstraeten, B. Schrauwen, J. Dambre, and P. Bienstman, "Experimental demonstration of reservoir computing on a silicon photonics chip," Nat. Commun. **5**, 4541 (2014).

[7] L. Appeltant, M. C. Soriano, G. Van der Sande, J. Danckaert, S. Massar, J. Dambre, B. Schrauwen, C. R. Mirasso, and I. Fischer, "Information processing using a single dynamical node as complex system," Nat. Commun. **2**, 468 (2011).

[8] L. Larger, M. C. Soriano, D. Brunner, L. Appeltant, J. M. Gutierrez, L. Pesquera, C. R. Mirasso, and I. Fischer, Photonic information processing beyond Turing: an optoelectronic implementation of reservoir computing," Opt. Express 20, 3241-3249 (2012).

[9] Y. Paquot, F. Duport, A. Smerieri, J. Dambre, B. Schrauwen, M. Haelterman, and S. Massar, "Optoelectronic reservoir computing," Sci. Rep. **2**, 287 (2012).

[10] R. Martinenghi, S. Rybalko, M. Jacquot, Y. K. Chembo, and L. Larger, "Photonic nonlinear transient computing with multiple-delay wavelength dynamics," Phys. Rev Lett. 108, 244101 (2012).

[11] F. Duport, B. Schneider, A. Smerieri, M. Haelterman, and Serge Massar, "All Optical Reservoir Computing," Optics Express **20**, 22783-22795 (2012).

[12] D. Brunner, M. C. Soriano, C. R. Mirasso, and I. Fischer, "Parallel photonic information processing at gigabyte per second data rates using transient states," Nature Commun., **4**, 1364 (2013).

[13] K. Hicke, M. A. Escalona-Moran, D. Brunner, M. C. Soriano, I. Fischer, and C. R. Mirasso, "Information processing using transient dynamics of semiconductor lasers subject to delayed feedback," IEEE J. Sel. Top. Quantum Electron. **19** 1501610 (2013).

[14] R. M. Nguimdo, G. Verschaffelt, J. Danckaert, and G. Van der Sande, "Fast photonic information processing using semiconductor lasers with delayed optical feedback: role of phase dynamics," Opt. Express **22**, 8673-8686 (2014).

[15] J. Dambre, D. Verstraeten, B. Schrauwen, and S. Massar, "Information processing capacity of dynamical systems," Sci. Rep. **2**, 514 (2012).

[16] I. V. Ermakov, G. Van der Sande and J. Danckaert, "Semiconductor ring laser subject to delayed optical feedback: bifurcations and stability", Commun. Nonlinear Sci. Numer. Simul. **17**, 4767 (2012).

[17] L. Mashal,G. Van der Sande, L. Gelens, J. Danckaert, and G. Verschaffelt, "Square-wave oscillations in semiconductor ring lasers with delayed optical feedback," Opt. Express. **20**, 22503-22516 (2012).

[18] R. M. Nguimdo, G. Verschaffelt, J. Danckaert, and G. Van der Sande, "Loss of time-delay signature in chaotic semiconductor ring lasers," Opt. Lett. **37**, 2541-2544 (2012).

[19] L. Mashal, R. M. Nguimdo,G. Van der Sande, M. C. Soriano, J. Danckaert, and G. Verschaffelt, "Low-frequency fluctuations in semiconductor ring lasers with optical feedback," IEEE J. Quantum Electron. **49**, 790-796 (2013).

[20] R. M. Nguimdo, G. Verschaffelt, J. Danckaert, X. Leijtens, J. Bolk, and G. Van der Sande, "Fast random bit generation based on a single chaotic semiconductor ring laser," Opt. Express **20**, 28603-28613 (2012)

[21] A. S. Weigend and N. A. Gershenfeld, "Time series prediction: Forecasting the future and understanding the past," ftp://ftp.santafe.edu/pub/Time-Series/Competition (1993).

[22] M. C. Soriano, S. Ortín, D. Brunner, L. Larger, C. R. Mirasso, I. Fischer, and L. Pesquera, "Optoelectronic reservoir computing: Tackling noise-induced performance degradation," Opt. Exp., **21**, 12 (2013).

[23] L. Appeltant, G. Van der Sande, J. Danckaert, and I. Fischer, "Constructing optimized binary masks for reservoir computing with delay systems," Sci. Rep. **4**, 3629 (2014).

[24] S. Sunada, T. Harayama, K. Arai, K. Yoshimura, K. Tsuzuki, A. Uchida, and P. Davis, "Random optical pulse generation with bistable semiconductor ring lasers," Opt. Express **19**, 7439-7450 (2011).